High-energy QCD phenomenology with next-to-leading order BFKL eigenfunctions

Speaker: Ada Polizzi, Università della Calabria, INFN - Cosenza

based on: A. Polizzi, M. Fucilla, A. Papa, Eur. Phys. J. C 85 (2025) 948

DIS 2026 - Bologna, Italy, 4-8 May

UNIVERSITÀ DELLA CALABRIA
DIPARTIMENTO DI FISICA

INFN
Gruppo Collegato di Cosenza
Istituto Nazionale di Fisica Nucleare

Overview

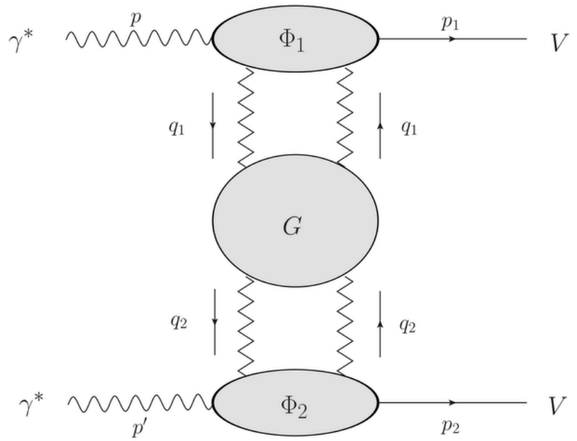

Theoretical background

- Introduction to BFKL;
- LO and NLO BFKL eigenfunctions.

Phenomenology-NLO eigenfunctions applications

- Electroproduction of two light vector mesons;
- Muller-Navelet jet production (preliminary results).

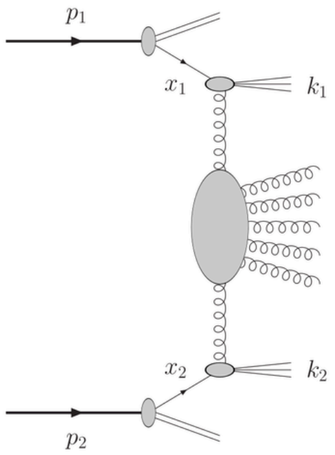

Conclusions and outlook

Theoretical background

Introduction to BFKL

$$x_{Bj} = \frac{Q^2}{s\,y}$$

Small-x regime

- PDF evolution is governed by DGLAP at fixed x.
- As s increases, smaller longitudinal momentum fractions become accessible.
- At small x, high-energy evolution is described by BFKL resummation (until saturation).
- Why is resummation necessary?

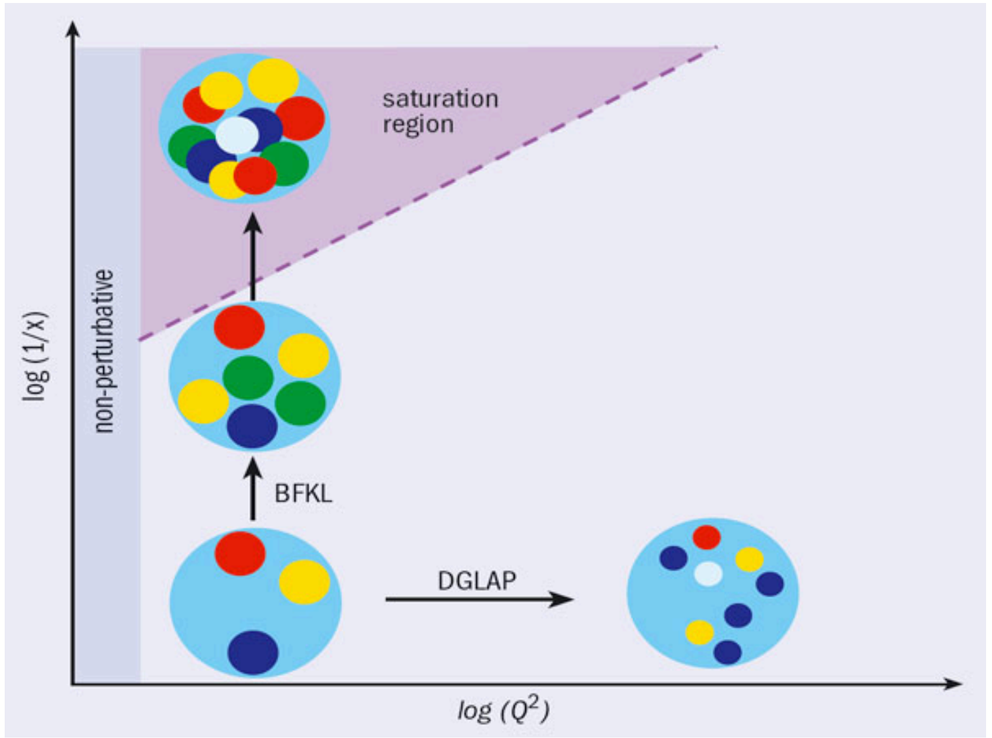

[cerncourier.com/a/qcd-scattering-from-dglap-to-bfkl/]

Semi-hard kinematical region

- Semi-hard regime $s \gg Q^2 \gg \lambda^2_{QCD}$.
- Dominance of gluon exchange in the t-channel.
- Real emitted gluons are strongly ordered in rapidity with similar transverse momenta (Multi-Regge kinematics).
- Rapidity gaps bring $\ln\left(\frac{s}{Q^2}\right)$ with each emission.
- Cross-section perturbative expansion is spoiled, BFKL resummation is needed.

$$\Delta y = \ln\left(\frac{s}{Q^2}\right)$$

Regge theory and the Pomeron

- High-energy amplitudes follow Regge behaviour.
- Dominance of a Reggeon exchange in the t-channel.
- Dominant total cross-section contributions come from vacuum exchange (Pomeron).
- Gluon Reggeizes in pQCD.
- Pomeron as a two-reggeized-gluon exchange in the t-channel.

$$\mathcal{A}(s,t) \sim s^{\alpha(t)}$$

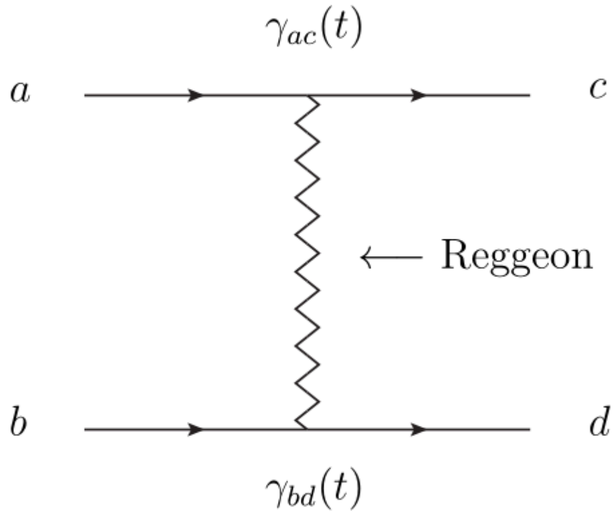

[**BFKL refs:** Fadin, Kuraev, Lipatov (1975); Kuraev, Lipatov, Fadin (1976-77); Balitsky, Lipatov (1978)]

BFKL factorization

- Reggized + real gluons → ladder
- Cross section factorizes in transverse momentum space.
- Green's function encodes universal evolution in rapidity.
- Transverse dynamics described by process-dependent impact factors.

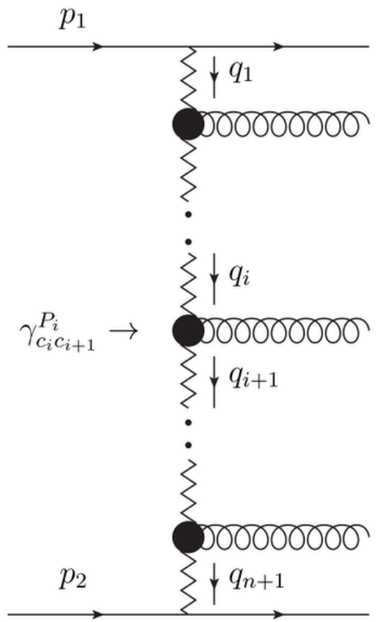

$$\Im m\mathcal{A} = \frac{s}{(2\pi)^2} \int \frac{d^2q_1}{\vec{q}_1^{\,2}} \int \frac{d^2q_2}{\vec{q}_2^{\,2}} \Phi_A\left(\vec{q}_1; s_0\right) \int_{\delta-i\infty}^{\delta+i\infty} \frac{d\omega}{2\pi i} \left[\left(\frac{s}{s_0}\right)^{\omega} G_\omega\left(\vec{q}_1, \vec{q}_2\right)\right] \Phi_B\left(-\vec{q}_2; s_0\right)$$

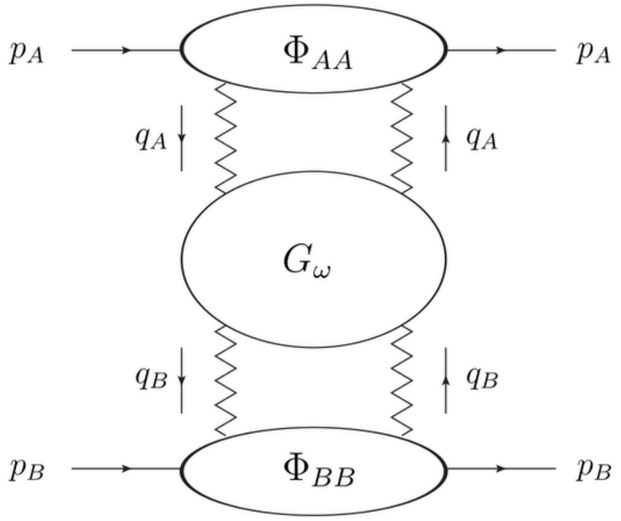

$$(\alpha_s \ln s)^n \rightarrow \text{LLA}$$

$$\alpha_s(\alpha_s \ln s)^n \rightarrow \text{NLLA}$$

BFKL equation and impact factors

- Green's function satisfies the BFKL equation:

$$\omega G_\omega(\vec{q}_1, \vec{q}_2) = \delta^{(2)}(\vec{q}_1 - \vec{q}_2) + \int d^2 q_r \, K(\vec{q}_1, \vec{q}_r) \, G_\omega(\vec{q}_r, \vec{q}_2)$$

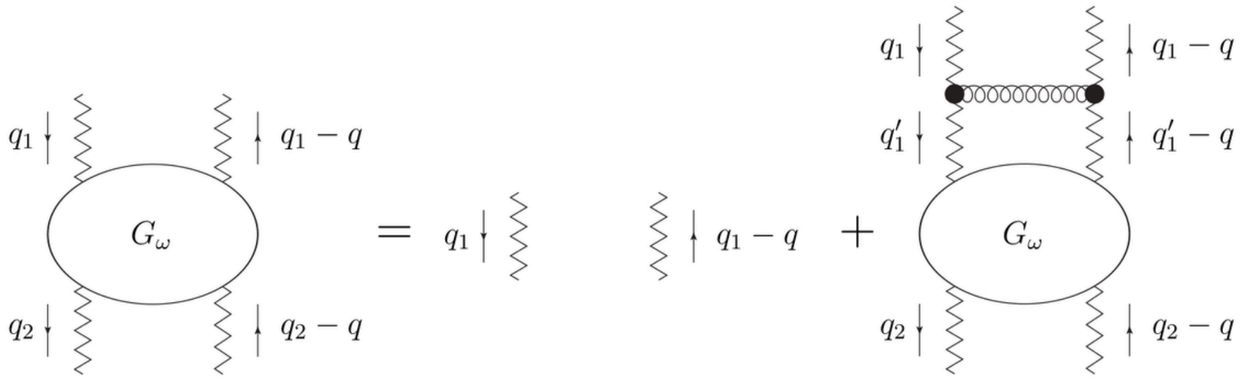

- Kernel includes real and virtual contributions.
- Operator solution: $\hat{G}_\omega = \dfrac{\hat{1}}{\omega - \hat{K}}$

- Asymptotics from rightmost ω-singularity, kernel eigenvalues control energy growth.
- Generic impact factor form: $\Phi_{AA'}(\vec{q_A}) = \dfrac{1}{\sqrt{N_c^2 - 1}} \sum_{\{f\}} \int \dfrac{ds_{PR}}{2\pi} \, d\rho_f \, \Gamma^c_{\{f\}A} \, \left(\Gamma^c_{\{f\}A'}\right)^*$

LO and NLO BFKL eigenfunctions

LO kernel eigenfunctions

- The LO BFKL kernel eigenvalue problem is exactly solvable.
- Eigenfunctions diagonalize the kernel in transverse momentum space.
- They form a complete basis labeled by $\nu \in \mathbb{R}$, $n \in \mathbb{Z}$.
- ν controls scaling, n is the conformal spin.
- The LO eigenvalue is given by the characteristic function $\chi(\nu, n)$.

$$\hat{K}^{(0)}|\nu^{(0)}, n\rangle = \chi(\nu, n)|\nu^{(0)}, n\rangle \qquad \chi(\nu, n) = 2\psi(1) - \psi\left(\frac{n+1}{2} + i\nu\right) - \psi\left(\frac{n+1}{2} - i\nu\right)$$

$$\langle \vec{q}|\nu^{(0)}, n\rangle = \frac{1}{\pi\sqrt{2}}\left(\vec{q}^{\,2}\right)^{i\nu-\frac{1}{2}} e^{in\theta}$$

NLO BFKL eigenfunctions

- The non-conformal NLO kernel is no longer diagonal in the LO basis.
- Eigenvalues and eigenfunctions are deformed perturbatively.
- Eigenfunctions acquire logarithmic distortions in $\vec{q}^2$.
- Singular behavior in ν must be treated with the distributional limit.
- Principal value prescription ensures well-defined integrals.

$$\hat{K}|\nu,n\rangle = \Delta(\nu,n)\,|\nu,n\rangle$$

$$\Delta(\nu,n) = \bar{\alpha}_s(\mu_R)\chi(\nu,n) + \bar{\alpha}_s^2(\mu_R)\chi_1(\nu,n)$$

$$\phi_{\nu,n}(\vec{q}) = \phi^{(0)}_{\nu,n}(\vec{q})\left[1 + \bar{\alpha}_s(\mu_R)h_{\nu,n}(\vec{q}^2)\right] \qquad h_{\nu,n}(\vec{q}^2) = A_{\nu,n}\ln^2\frac{\vec{q}^2}{\mu_R^2} + B_{\nu,n}\ln\frac{\vec{q}^2}{\mu_R^2}$$

$$A_{\nu,n} = i\,\frac{\beta_0}{8N_c}\,\frac{\chi(\nu,n)}{\chi'(\nu,n)}\,, \qquad B_{\nu,n} = \frac{\beta_0}{8N_c}\,\frac{d}{d\nu}\left(\frac{\chi(\nu,n)}{\chi'(\nu,n)}\right)$$

[G. A. Chirilli, Y. V. Kovchegov, JHEP 06 (2013) 055]

From eigenfunctions to LLA amplitudes

- Eigenfunctions allow spectral decomposition of the Green's function.
- Impact factors project external states onto the eigenbasis.
- LLA corresponds to LO eigenfunctions + LO kernel.

$$\Im m_s \mathcal{A}\Big|_{\text{LLA}} = \frac{s}{(2\pi)^2}\int_{\delta-i\infty}^{\delta+i\infty}\frac{d\omega}{2\pi i}\left(\frac{s}{s_0}\right)^{\omega}\ \langle\Phi_A^{(0)}\mid\frac{1}{\hat{\vec{q}}^2}\ \frac{\hat{1}}{\omega-\bar{\alpha}_s\hat{K}^{(0)}}\ \frac{1}{\hat{\vec{q}}^2}\ |\Phi_B^{(0)}\rangle$$

$$= \frac{s}{(2\pi)^2}\sum_{n=-\infty}^{+\infty}\int_{-\infty}^{+\infty}d\nu\ \left(\frac{s}{s_0}\right)^{\bar{\alpha}_s\chi(\nu,n)}\ \alpha_s^2\ c_1(\nu,n)\,c_2(\nu,n)$$

$$c_1(\nu,n) = \langle\Phi_A^{(0)}|\frac{1}{\hat{\vec{q}}^2}|\nu^{(0)},n\rangle$$

$$c_2(\nu,n) = \langle\nu^{(0)},n|\frac{1}{\hat{\vec{q}}^2}|\Phi_B^{(0)}\rangle$$

NLLA amplitudes via LO eigenfunctions

- NLLA introduces corrections in both kernel and impact factors.
- At NLLA, LO eigenfunctions are no longer exact eigenstates.
- Kernel develops diagonal and non-diagonal contributions.
- Non-diagonal terms generate derivative operators in $\boldsymbol{\nu}$.

$$\hat{K}|\nu^{(0)}\rangle = \bar{\alpha}_s\chi(\nu)|\nu^{(0)}\rangle + \bar{\alpha}_s^2\chi^{(1)}(\nu)|\nu^{(0)}\rangle + \bar{\alpha}_s^2\frac{\beta_0}{4N_c}\chi(\nu)\, i\frac{\partial}{\partial\nu}|\nu^{(0)}\rangle$$

NNLLA contributions

NLO IF corrections onto LO eigenbasis

$$\Im m_s\mathcal{A}\Big|_{\text{NLLA}} = \frac{s}{(2\pi)^2}\int_{-\infty}^{+\infty} d\nu \left(\frac{s}{s_0}\right)^{\bar{\alpha}_s(\mu_R)\chi(\nu)} \alpha_s^2\; c_1(\nu)c_2(\nu)$$

$$\times\left[1+\bar{\alpha}_s(\mu_R)\left(\frac{c_1^{(1)}(\nu)}{c_1(\nu)}+\frac{c_2^{(1)}(\nu)}{c_2(\nu)}\right)\right.$$

$$\left.+\bar{\alpha}_s^2(\mu_R)\ln\left(\frac{s}{s_0}\right)\left(\bar{\chi}(\nu)+\frac{\beta_0}{8N_c}\chi(\nu)\left[-\chi(\nu)+\frac{10}{3}+i\frac{d\ln(\frac{c_1(\nu)}{c_2(\nu)})}{d\nu}+2\ln\mu_R^2\right]\right)\right]$$

NLLA amplitudes via NLO eigenfunctions

$$\text{LO basis} \iff \text{NLO eigenfunction basis at NLLA}$$

- NLO eigenfunctions diagonalize the kernel.
- IF projection on the NLO eigenbasis.
- Amplitudes via different basis are equivalent to NLLA accuracy (verified general property).
- Differences appear only beyond NLLA.
- This freedom is useful for phenomenology and stability.

$$\Im m_s \mathcal{A}\Big|_{\text{NLLA}} = \frac{s}{(2\pi)^2} \int_{-\infty}^{+\infty} d\nu \left(\frac{s}{s_0}\right)^{\bar{\alpha}_s \chi(\nu) + \bar{\alpha}_s^2 \chi_1(\nu)} \alpha_s^2 \; \tilde{c}_1(\nu)\tilde{c}_2(\nu) \left[1 + \bar{\alpha}_s \left(\frac{c_1^{(1)}(\nu)}{\tilde{c}_1(\nu)} + \frac{c_2^{(1)}(\nu)}{\tilde{c}_2(\nu)}\right)\right]$$

$$\tilde{c}_{1,2}(\nu) = c_{1,2}(\nu) + \mathcal{O}(\bar{\alpha}_s)$$

Phenomenology-NLO eigenfunctions applications

Electroproduction of two light vector mesons

LO vs NLO basis

- Study of the forward production with equal virtualities.
- Leading-twist IF encoding transitions between longitudinally polarized states are known at NLO.
- Two NLLA formulations: via LO and NLO basis.
- Different beyond-NLLA terms affects the dependence on s_0 and μ_R.
- Comparison tests the practical impact of the NLO eigenfunctions.

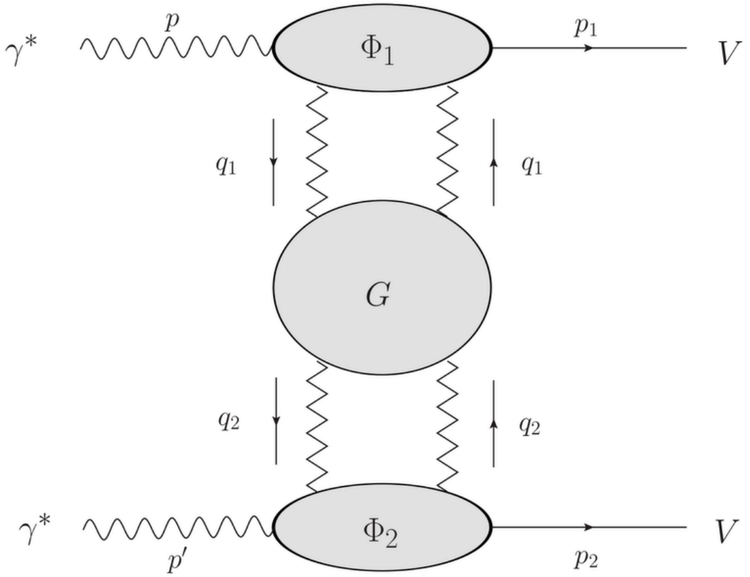

$$\gamma^*(p)\,\gamma^*(p') \to V(p_1)\,V(p_2)\;, V = \rho^0, \omega, \phi$$

$$\Phi_{1,2}(\vec{q}) = \alpha_s\, D_{1,2}\left[C^{(0)}_{1,2}(\vec{q}^{\,2}) + \bar{\alpha}_s C^{(1)}_{1,2}(\vec{q}^{\,2})\right]$$

Standard representation

- Numerical scans are performed over $Y_0 = \ln\left(\frac{s_0}{Q^2}\right), \frac{\mu_R}{Q}$ at $Q^2 = 24\,\mathrm{GeV}^2$ selecting stability-scales (PMS).
- In the LO basis (A_0), stability appears only at large Y_0 and μ_R.
- Natural settings $Y_0 = 0, \mu_R = Q$ can lead to large negative values.
- In the NLO basis (A_1), a maximum appears near more physical scales.

$$\frac{Q^2}{D_1 D_2}\frac{\Im m_s \mathcal{A}_0}{s} = \frac{Q^2}{(2\pi)^2}\alpha_s^2 \times \int_{-\infty}^{+\infty} d\nu \left(\frac{s}{s_0}\right)^{\bar{\alpha}_s(\mu_R)\chi(\nu)} c_1(\nu)c_2(\nu)\left[1 + \bar{\alpha}_s(\mu_R)\left[\ln\left(\frac{s_0}{Q^2}\right)\chi(\nu) + \frac{\beta_0}{2N_c}\left(\ln\left(\frac{\mu_R^2}{Q^2}\right) + f(\nu)\right) + \frac{\bar{c}_1^{(1)}(\nu)}{c_1(\nu)} + \frac{\bar{c}_2^{(1)}(\nu)}{c_2(\nu)}\right] + \bar{\alpha}_s^2(\mu_R)\ln\left(\frac{s}{s_0}\right) \times \left(\bar{\chi}(\nu) + \frac{\beta_0}{8N_c}\chi(\nu)\left[-\chi(\nu) + \frac{10}{3} + i\frac{d\ln(\frac{c_1(\nu)}{c_2(\nu)})}{d\nu} + 2\ln\mu_R^2\right]\right)\right]$$

$$\frac{Q^2}{D_1 D_2}\frac{\Im m_s \mathcal{A}_1}{s} = \frac{Q^2}{(2\pi)^2}\alpha_s^2 \times \int_{-\infty}^{+\infty} d\nu \left(\frac{s}{s_0}\right)^{\bar{\alpha}_s(\mu_R)\chi(\nu)+\bar{\alpha}_s^2\chi_1(\nu)} c_1(\nu)c_2(\nu)\left[1 + \bar{\alpha}_s(\mu_R)\left(A_\nu\left(f_1(\nu) - 2\ln\left(\frac{\mu_R^2}{Q^2}\right)f_2(\nu)\right) + B_\nu\left(-2\left(f(\nu) - \frac{5}{3}\right) - 2\ln\left(\frac{\mu_R^2}{Q^2}\right)\right) + \frac{\bar{c}_1^{(1)}(\nu)}{\tilde{c}_1(\nu)} + \frac{\bar{c}_2^{(1)}(\nu)}{\tilde{c}_2(\nu)} + f_3(\nu)\right)\right]$$

Standard representation

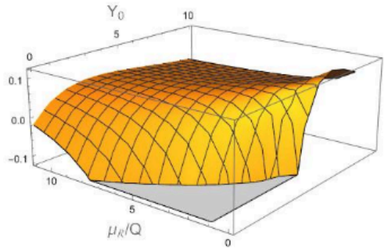

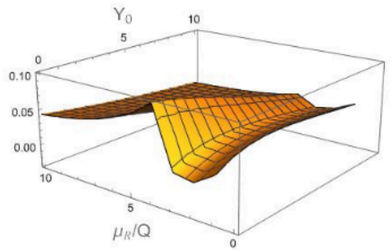

For $Y = 10$, $\mathcal{I}m_s(\mathcal{A}_0)Q^2/(s\,D_1D_2)$ on the left and $\mathcal{I}m_s(\mathcal{A}_1)Q^2/(s\,D_1D_2)$ on the right.

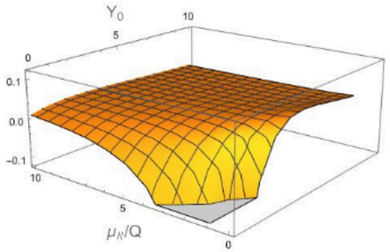

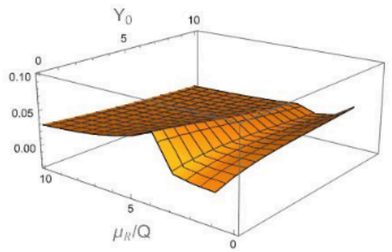

For $Y = 6$, $\mathcal{I}m_s(\mathcal{A}_0)Q^2/(s\,D_1D_2)$ on the left and $\mathcal{I}m_s(\mathcal{A}_1)Q^2/(s\,D_1D_2)$ on the right.

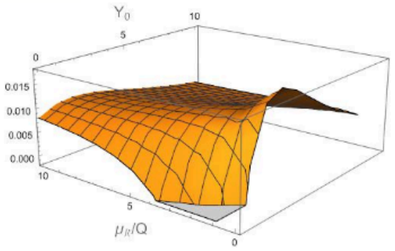

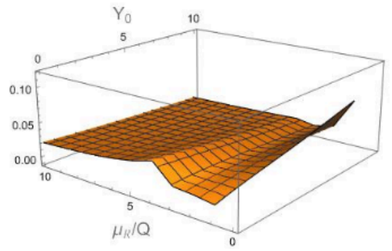

For $Y = 2$, $\mathcal{I}m_s(\mathcal{A}_0)Q^2/(s\,D_1D_2)$ on the left and $\mathcal{I}m_s(\mathcal{A}_1)Q^2/(s\,D_1D_2)$ on the right.

Series representation

- Recasting of both amplitudes into a series representation.
- This makes explicit the resummation of leading and next-to-leading logs.
- The structure is common to both bases.
- Leading-log coefficients are universal.
- Basis dependence enters only through subleading terms.

$$\frac{Q^2}{D_1 D_2}\frac{\Im m_s \mathcal{A}_{0,1}}{s} = \frac{1}{(2\pi)^2}\alpha_s^2$$

$$\times\left[b_0 + \sum_{n=1}^{\infty} \bar{\alpha}_s^n\, b_n \left(\ln\left(\frac{s}{s_0}\right)^n + d_n(s_0,\mu)\ln\left(\frac{s}{s_0}\right)^{n-1}\right)\right]$$

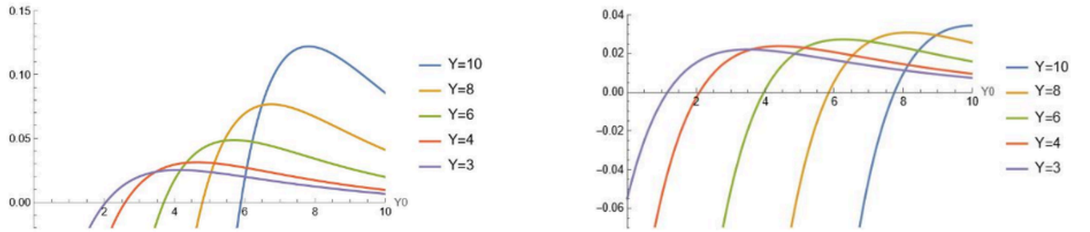

For $\mu_r = Q$, $\mathcal{I}m_s(\mathcal{A}_0)Q^2/(s\,D_1D_2)$ on the left and $\mathcal{I}m_s(\mathcal{A}_1)Q^2/(s\,D_1D_2)$ on the right.

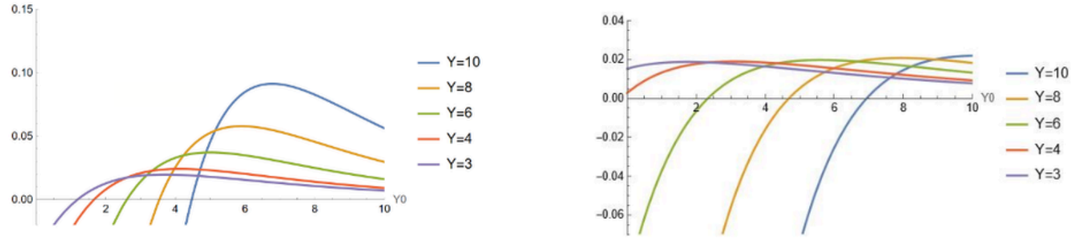

For $\mu_r = 2Q$, $\mathcal{I}m_s(\mathcal{A}_0)Q^2/(s\,D_1D_2)$ on the left and $\mathcal{I}m_s(\mathcal{A}_1)Q^2/(s\,D_1D_2)$ on the right.

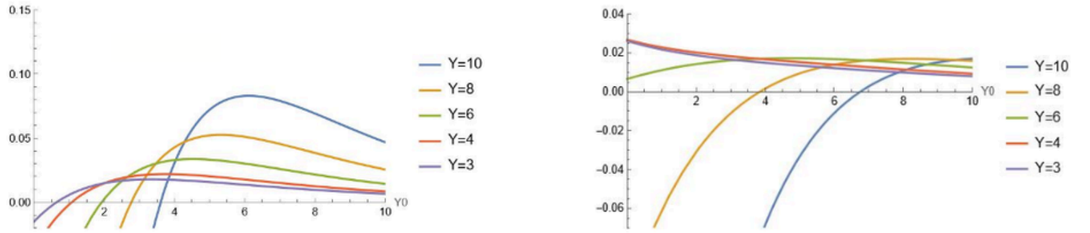

For $\mu_r = 3Q$, $\mathcal{I}m_s(\mathcal{A}_0)Q^2/(s\,D_1D_2)$ on the left and $\mathcal{I}m_s(\mathcal{A}_1)Q^2/(s\,D_1D_2)$ on the right.

Muller-Navelet jets

LO vs NLO basis (preliminary results)

- Well suited for BFKL due to their large jet-rapidity separation.
- Azimuthal correlations highly sensitive probes of high-energy QCD dynamics.
- LLA overestimates decorrelation and suffers from strong scale instabilities; NLLA restores reliable shape of the correlation spectra and improves stability.

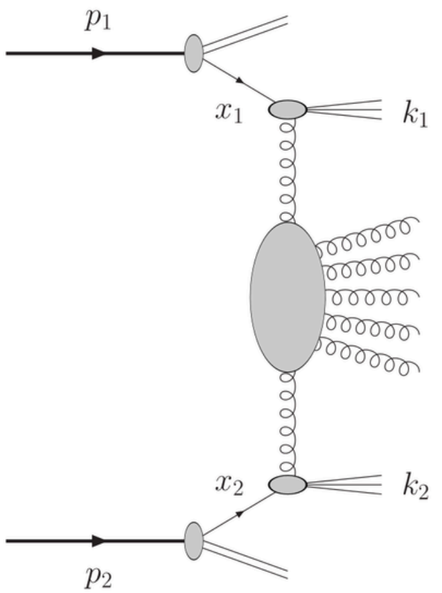

$$\frac{d\sigma}{dy_1\,dy_2\,d|\vec{k}_1|\,d|\vec{k}_2|d\phi_1\,d\phi_2} = \frac{d\Phi_1}{dy_1\,d|\vec{k}_1|d\phi_1} \otimes G \otimes \frac{d\Phi_2}{dy_2\,d|\vec{k}_2|d\phi_2}$$
$$= \frac{1}{(2\pi)^2}\left[C_0 + \sum_{n=1}^{\infty} 2\cos(n\phi)\,C_n\right], \quad \phi = \phi_1 - \phi_2 - \pi$$

$$p(p_1) + p(p_2) \to \mathrm{jet}(k_{J_1}) + \mathrm{jet}(k_{J_2}) + X$$

[Mueller-Navelet (1987); Colferai-Vacca and collaborators (2000-2010s); Ducloué-Szymanowski-Wallon (2013-2015)]

- Azimuthal correlations: $\langle \cos(n\phi) \rangle = \mathcal{C}_n / \mathcal{C}_0$.
- Initial parameters: rapidity difference $Y = 6, \mu_R = \mu_F, \sqrt{s} = 14\,\mathrm{TeV}, |\vec{k}_{J_1}| = |\vec{k}_{J_2}| = 35\,\mathrm{GeV}, n = 1.$
- Azimuthal correlation evaluated with: LO basis, standard representation $\mathcal{C}_n$, LO basis, exponential representation $\mathcal{C}_n^{\exp}$, NLO basis $\mathcal{C}_n^{\mathrm{NLO}}$.

$$\mathcal{C}_n = \frac{x_{J_1} x_{J_2}}{|\vec{k}_{J_1}||\vec{k}_{J_2}|} \int_{-\infty}^{+\infty} d\nu \left(\frac{x_{J_1} x_{J_2} s}{s_0}\right)^{\bar{\alpha}_s(\mu_R)\chi(n,\nu)}$$
$$\times \alpha_s^2(\mu_R) c_1(n,\nu,|\vec{k}_{J_1}|,x_{J_1}) c_2(n,\nu,|\vec{k}_{J_2}|,x_{J_2})$$
$$\times \left[1 + \alpha_s(\mu_R)\left(\frac{c_1^{(1)}(n,\nu,|\vec{k}_{J_1}|,x_{J_1})}{c_1(n,\nu,|\vec{k}_{J_1}|,x_{J_1})} + \frac{c_2^{(1)}(n,\nu,|\vec{k}_{J_2}|,x_{J_2})}{c_2(n,\nu,|\vec{k}_{J_2}|,x_{J_2})}\right)\right.$$
$$\left. + \bar{\alpha}_s^2(\mu_R) \ln\left(\frac{x_{J_1} x_{J_2} s}{s_0}\right)\left(\bar{\chi}(n,\nu) + \frac{\beta_0}{8C_A}\chi(n,\nu)\left(-\chi(n,\nu) + \frac{10}{3} + \ln\frac{\mu_R^4}{\vec{k}_{J_1}^2 \vec{k}_{J_2}^2}\right)\right)\right]$$

$$\mathcal{C}_n^{\exp} = \frac{x_{J_1} x_{J_2}}{|\vec{k}_{J_1}||\vec{k}_{J_2}|} \int_{-\infty}^{+\infty} d\nu \exp\left[(Y - Y_0)\left(\bar{\alpha}_s(\mu_R)\chi(n,\nu)\right.\right.$$
$$\left.\left. + \bar{\alpha}_s^2(\mu_R)\left(\bar{\chi}(n,\nu) + \frac{\beta_0}{8C_A}\chi(n,\nu)\left(-\chi(n,\nu) + \frac{10}{3} + \ln\frac{\mu_R^4}{\vec{k}_{J_1}^2 \vec{k}_{J_2}^2}\right)\right)\right)\right]$$
$$\times \alpha_s^2(\mu_R) c_1(n,\nu,|\vec{k}_{J_1}|,x_{J_1},\mu_F) c_2(n,\nu,|\vec{k}_{J_2}|,x_{J_2},\mu_F)$$
$$\times \left[1 + \alpha_s(\mu_R)\left(\frac{c_1^{(1)}(n,\nu,|\vec{k}_{J_1}|,x_{J_1},\mu_F)}{c_1(n,\nu,|\vec{k}_{J_1}|,x_{J_1},\mu_F)} + \frac{c_2^{(1)}(n,\nu,|\vec{k}_{J_2}|,x_{J_2},\mu_F)}{c_2(n,\nu,|\vec{k}_{J_2}|,x_{J_2},\mu_F)}\right)\right]$$

[F. Caporale, D. Yu. Ivanov, B. Murdaca, A. Papa, Nucl. Phys. B 877 (2013) 73-94]

$$\mathcal{C}_n^{\mathrm{NLO}} = \frac{x_{J_1} x_{J_2}}{|\vec{k}_{J_1}||\vec{k}_{J_2}|} \int_{-\infty}^{+\infty} d\nu \exp\left[(Y - Y_0)\Delta(\nu,n)\right]$$
$$\times \alpha_s^2(\mu_R) c_1(n,\nu,|\vec{k}_{J_1}|,x_{J_1},\mu_F) c_2(n,\nu,|\vec{k}_{J_2}|,x_{J_2},\mu_F)$$
$$\times \left[1 + \bar{\alpha}_s(\mu_R)\left(I_1(\nu,n,|\vec{k}_{J_1}|) + I_2(\nu,n,|\vec{k}_{J_2}|)\right)\right.$$
$$\left. + \alpha_s(\mu_R)\left(\frac{c_1^{(1)}(n,\nu,|\vec{k}_{J_1}|,x_{J_1},\mu_F)}{c_1(1 + \bar{\alpha}_s(\mu_R) I_1)} + \frac{c_2^{(1)}(n,\nu,|\vec{k}_{J_2}|,x_{J_2},\mu_F)}{c_2(1 + \bar{\alpha}_s(\mu_R) I_2)}\right)\right]$$

New result

- Predictions in the NLO basis remain more bounded under parameter variations.
- However, the best stabilization in the natural-parameter region is achieved with LO basis, exponential representation.
- Chernyshev, A. A.; Nefedov, M. A.; Saleev, V. A., arXiv:2506.10458 [hep-ph] (2025): a combination of BFKL NLO basis, HEF and Sudakov resummation is needed for optimization without scale setting (PMS, BLM).

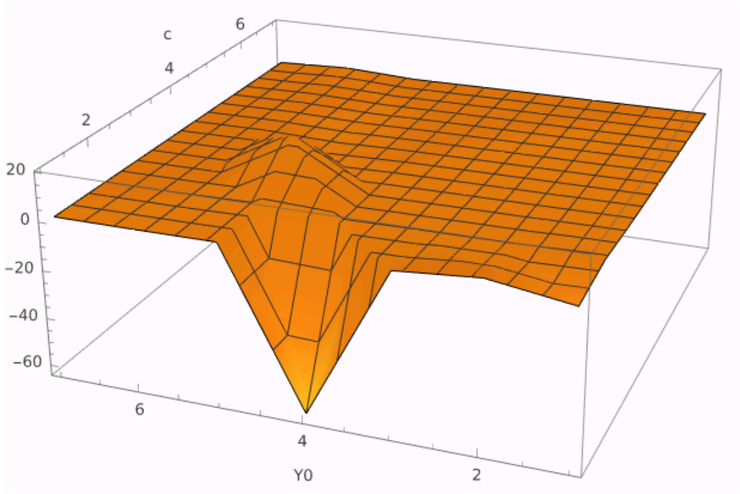

C_1/C_0

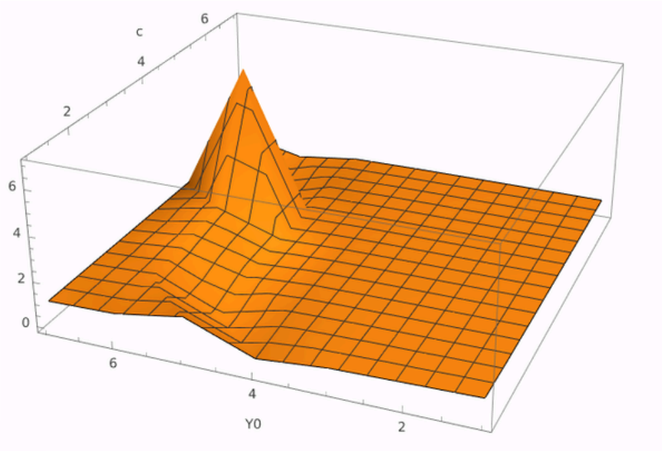

$C_1^{\exp}/C_0^{\exp}$

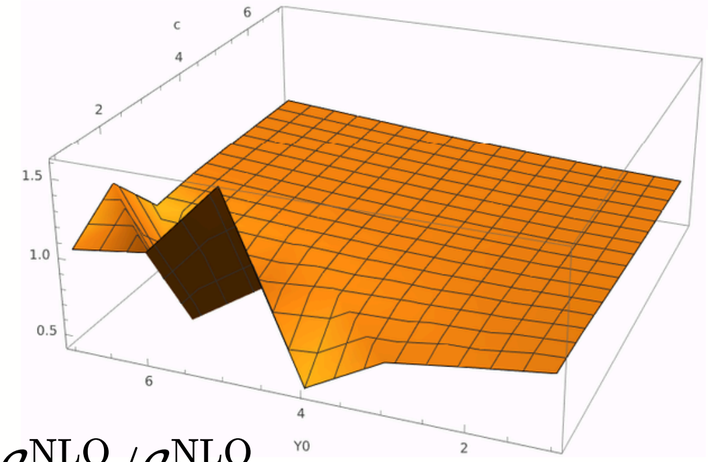

$C_1^{\mathrm{NLO}}/C_0^{\mathrm{NLO}}$

New result

Conclusions and outlook

- Process independent **equivalence** between the two-basis NLLA formulation is provided.
- Phenomenological impact of the NLO basis must be assessed **case by case**.
- **Advancing phenomenology:** consistent formulation for mesons electroproduction, improvements needed for M-N jets

→

- **Collinear improvement** for mesons electroproduction.
- Retrieving experimental M-N jets azimuthal correlations with optimized scales from **NLO BFKL + HEF + Sudakov resummation.**
- **Application to other processes** (DIS Forward jet production, Di-hadron production, Heavy-quark pair production (EIC), etc.)

Thank You!

Backup

BFKL at NLLA

- BFKL violates unitarity and cannot be applied at asymptotically high energies; saturation effects are required.
- Sub-leading effects can improve stability within the linear formulation.
- Moreover, s_0 and μ_R are not fixed in the LLA → NLLA

$$\sigma_{tot}^{LLA} \sim \frac{s^{\omega_0}}{\sqrt{\ln s}}$$

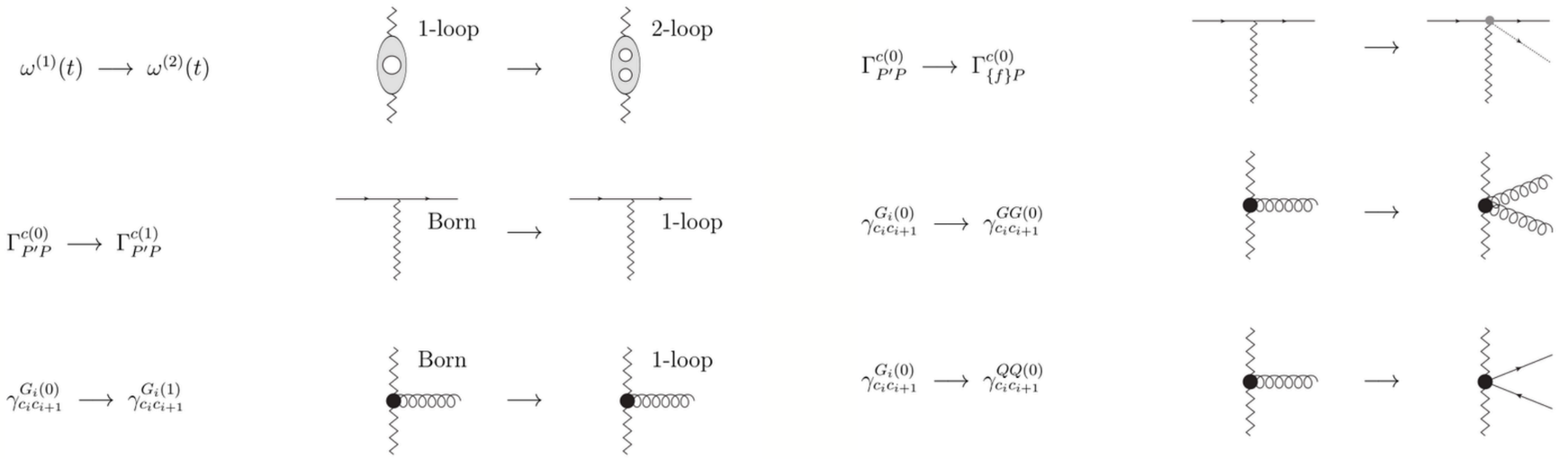

Quasi Multi-Regge-Kinematics

Equivalence between NLLA amplitudes

$$\tilde{c}_1(\nu) = \left\{1 + \bar{\alpha}_s \left[A_\nu \left(-i\frac{d}{d\nu} - \ln \mu_R^2\right)^2 + B_\nu \left(-i\frac{d}{d\nu} - \ln \mu_R^2\right)\right]\right\} c_1(\nu) \,,$$

$$\tilde{c}_2(\nu) = \left\{1 + \bar{\alpha}_s \left[-A_\nu \left(+i\frac{d}{d\nu} - \ln \mu_R^2\right)^2 + B_\nu \left(+i\frac{d}{d\nu} - \ln \mu_R^2\right)\right]\right\} c_2(\nu)$$

$\longrightarrow$

$$\Im m_s \mathcal{A}^{\mathrm{NLO}}\Big|_{\mathrm{NLLA}} = \frac{s}{(2\pi)^2} \int_{-\infty}^{+\infty} d\nu \left(\frac{s}{s_0}\right)^{\bar{\alpha}_s \chi(\nu) + \bar{\alpha}_s{}^2 \chi_1(\nu)} \alpha_s^2 \, c_1(\nu) c_2(\nu)$$
$$\times \left[1 + \bar{\alpha}_s \left(\frac{c_1^{(1)}(\nu)}{c_1(\nu)} + \frac{c_2^{(1)}(\nu)}{c_2(\nu)}\right)\right.$$
$$\left. + \bar{\alpha}_s \left(-A_\nu \left(\frac{c_1''(\nu)}{c_1(\nu)} - \frac{c_2''(\nu)}{c_2(\nu)}\right) - iB_\nu \frac{d \ln\left(\frac{c_1(\nu)}{c_2(\nu)}\right)}{d\nu} + 2 \ln \mu_R^2 \left(iA_\nu \frac{d \ln c_1(\nu) c_2(\nu)}{d\nu} - B_\nu\right)\right)\right]$$

$$I = \int_{-\infty}^{+\infty} d\nu \left(\frac{s}{s_0}\right)^{\bar{\alpha}_s \chi} c_1 c_2 \left[i\frac{\chi}{\chi'}\left(\frac{c_2''}{c_2} - \frac{c_1''}{c_1}\right) - i\frac{d}{d\nu}\left(\frac{\chi}{\chi'}\right)\frac{d}{d\nu}\ln\frac{c_1}{c_2}\right.$$
$$\left. - 2\ln\mu_R^2 \left(\frac{\chi}{\chi'}\frac{d}{d\nu}\ln(c_1 c_2) + \frac{d}{d\nu}\left(\frac{\chi}{\chi'}\right)\right)\right]$$

$$J = \int_{-\infty}^{+\infty} d\nu \left(\frac{s}{s_0}\right)^{\bar{\alpha}_s \chi} c_1 c_2 \, \bar{\alpha}_s \, \chi \, \ln\left(\frac{s}{s_0}\right)\left(i\frac{d}{d\nu}\ln\frac{c_1}{c_2} + 2\ln\mu_R^2\right)$$

Equivalence if I and J coincide

$\longrightarrow$

It can be shown using

$$c_1 c_2 \left[\frac{\chi}{\chi'}\left(\frac{c_2''}{c_2} - \frac{c_1''}{c_1}\right) - \frac{d}{d\nu}\left(\frac{\chi}{\chi'}\right)\frac{d}{d\nu}\ln\frac{c_1}{c_2}\right] = -\frac{d}{d\nu}\left(c_1 c_2 \frac{\chi}{\chi'}\frac{d}{d\nu}\ln\frac{c_1}{c_2}\right),$$

$$c_1 c_2 \left[\frac{\chi}{\chi'}\frac{d}{d\nu}\ln(c_1 c_2) + \frac{d}{d\nu}\left(\frac{\chi}{\chi'}\right)\right] = \frac{d}{d\nu}\left(c_1 c_2 \frac{\chi}{\chi'}\right),$$

$$\int_{-\infty}^{+\infty} d\nu \left(\frac{s}{s_0}\right)^{\bar{\alpha}_s \chi} \bar{\alpha}_s \ln\left(\frac{s}{s_0}\right) f(\nu) = \int_{-\infty}^{+\infty} d\nu \left(\frac{s}{s_0}\right)^{\bar{\alpha}_s \chi} \bar{\alpha}_s \ln\left(\frac{s}{s_0}\right) f(\nu) \, \chi' P \frac{1}{\chi'}$$
$$= -\int_{-\infty}^{+\infty} d\nu \left(\frac{s}{s_0}\right)^{\bar{\alpha}_s \chi} \frac{d}{d\nu}\left(P \frac{f(\nu)}{\chi'(\nu)}\right)$$

Numerical implementation of NLO eigenfunctions

- Mesons electroproduction numerical implementation:

$$P\frac{1}{\chi'(\nu)} \to \mathcal{R}e\left[\frac{1}{\chi'(\nu)+i\epsilon}\right], \quad \frac{d}{d\nu}\left(P\frac{1}{\chi'(\nu)}\right) \to -\mathcal{R}e\left[\frac{\chi''(\nu)}{(\chi'(\nu)+i\epsilon)^2}\right]$$

- In the M-N jets numerical implementation, double pole treated with the Hadamard regularization:

$$\mathrm{Fp}\int_{-\infty}^{\infty}\frac{\varphi(x)}{x^2}\,dx = \lim_{\epsilon\to 0}\left[\int_{-\infty}^{-\epsilon}\frac{\varphi(x)}{x^2}\,dx + \int_{\epsilon}^{\infty}\frac{\varphi(x)}{x^2}\,dx - \frac{2\varphi(0)}{\epsilon}\right]$$

$$\downarrow$$

$$2\int_0^{10}\frac{\chi''(\nu)(\rho(\nu)-\rho(0))}{\chi'(\nu)^2}\,dx - 2\frac{\rho(0)}{\chi'(10)}$$

using parity

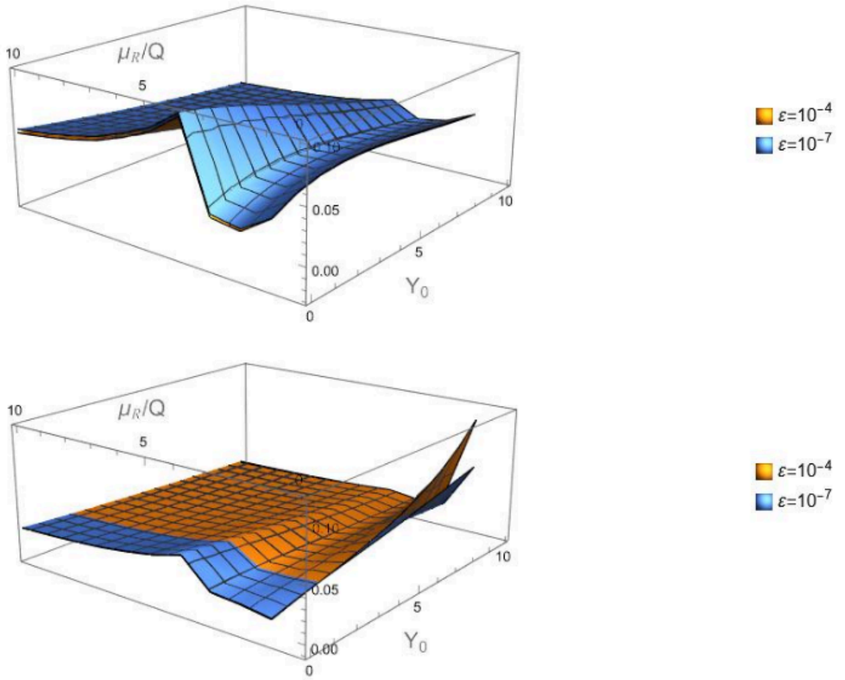

$\mathcal{I}m_s(\mathcal{A}_1)Q^2/(s\,D_1D_2)$ with $\epsilon = 10^{-4}, 10^{-7}$; for $Y = 10$ (up) and $Y = 2$ (down), at $Q^2 = 24$ GeV^2.